miR-376c-3p modulates the properties of breast cancer stem cells by targeting RAB2A

FENG ZHAO*, MING ZHONG*, WENJIANG PEI, BAOXING TIAN and YANTAO CAI

Department of General Surgery, Shanghai Ninth People's Hospital Affiliated to Shanghai Jiao Tong University School of Medicine, Shanghai 200011, P.R. China

Received April 8, 2019; Accepted July 21, 2020

DOI: 10.3892/etm.2020.9196

Abstract. MicroRNAs (miRNAs/miRs) negatively regulate gene expression and participate in various cellular processes. miRNA dysregulation is associated with cancer progression. The present study aimed to identify the miRNAs that participate in breast cancer tumorigenesis and determine the mechanism that underlies this. miRNA microarray data analysis and validation assays indicated that miR-376c-3p was downregulated in breast tumour tissues and breast cancer stem cells (BCSCs) compared with adjacent non-cancerous tissues and MCF-10A cells, respectively. Ras-related protein Rab-2A (RAB2A) was predicted as a target of miR-376c-3p, which was confirmed by conducting further experiments. miR-376c-3p regulated the BCSC population and the expression of stem cell regulatory genes by targeting RAB2A. By performing mammosphere, Cell Counting Kit-8, colony formation and transwell invasion assays, it was demonstrated that miR-376c-3p also inhibited BCSC self-renewal, proliferation and invasion by regulating RAB2A expression. Using a xenograft mouse model, it was revealed that miR-376c-3p overexpression suppressed breast cancer growth *in vivo*. In conclusion, the results indicated that miR-376c-3p targeted RAB2A to regulate BCSC fate and properties; therefore, miR-376c-3p may serve as a potential therapeutic target for breast cancer.

Correspondence to: Dr Yantao Cai, Department of General Surgery, Shanghai Ninth People's Hospital Affiliated to Shanghai Jiao Tong University School of Medicine, 639 Zhizaoju Road, Huangpu, Shanghai 200011, P.R. China
E-mail: yantaocaidfr@163.com

*Contributed equally

Abbreviations: miRNAs, microRNAs; BCSCs, breast cancer stem cells; CSCs, cancer stem cells; GEO, Gene Expression Omnibus; IHC, immunohistochemistry

Key words: miR-376c-3p, Ras-related protein Rab-2A, BCSCs

Introduction

Tumour heterogeneity has been considered as an obstacle for curing cancers. Among the hierarchically organized tumours, exist a small portion of cancer cells that display stem cell properties, which are termed cancer stem cells (CSCs) (1). CSCs are essential for cancer development, with self-renewal, differentiation, tumorigenesis and chemoresistance properties (1,2).

Breast cancer is the most frequently occurring cancer in women, causing the highest number of cancer-related deaths in females worldwide (3). In 2018, 15% of all cancer-related deaths in females were caused by breast cancer (4,5). Breast cancer stem cells (BCSCs), which can be identified as cluster of differentiation (CD)44^+CD24^- cells, are thought to be responsible for the origin, metastasis and drug resistance of breast cancer (6). Understanding the regulatory mechanism underlying BCSCs may be beneficial for developing improved therapeutic strategies for breast cancer.

MicroRNAs (miRNAs/miRs) are a class of small, non-coding RNAs that are ~20 nucleotides in length (7,8). By binding to the 3'-untranslated region of target mRNAs by complementary base-pairing, miRNAs can induce target mRNA degradation and translation suppression, thereby negatively regulating gene expression (7,8). miRNA dysregulation has been reported in a number of different types of cancer (7). miRNAs serve important regulatory roles in cancer initiation and development, affecting the fate of CSCs (8-10). miRNAs Let-7 (11), miR-200c (12,13), miR-93 (14), miR-203 (15) and mi-600 (16) have been reported to modulate the properties of BCSCs. The fate of other CSCs, such as liver (17), prostate (18), colorectal (19,20) and glioblastoma (21) CSCs, has also been linked to miRNAs.

miR-376c-3p has been implicated in signalling pathways that modulate cancer procession. miR-376c-3p has been identified as a cancer suppressor in head and neck squamous cancer via targeting of RUNX family transcription factor 2 (RUNX2) and suppressing RUNX2-mediated metastasis (22). Moreover, miR-376c-3p negatively regulates gastric tumour growth by modulating the expression of BCL2 associated agonist of cell death (BAD) and Smad4 (23). miR-376c-3p also suppresses cell proliferation and induces apoptosis in oral squamous cancer cells and neuroblastoma cells by targeting homeobox B7 (24) and Cyclin D1 (25), respectively. However, another study reported that miR-376c-3p facilitates hepatocellular carcinoma

progression by inhibiting AT-rich interaction domain 2 expression (26). miR-367c-3p was also reported to enhance cell viability and inhibit apoptosis in colorectal cancer cells (27).

Ras-related protein Rab-2A(RAB2A) is a small GTPase that has been identified as an oncogene in breast cancer (28,29). The present study suggested that miR-376c-3p was downregulated in breast cancer by conducting a miRNA microarray analysis. RAB2A was predicted as a target of miR-376c-3p via online software TargetScan. Moreover, the expression level of miR-376c-3p was negatively correlated with the expression level of RAB2A in breast cancer tumours. Further investigation demonstrated that miR-376c-3p inhibited BCSC fate and properties by targeting RAB2A.

Materials and methods

Tumour samples. A total of 60 paired breast tumour samples and adjacent non-tumorous tissues (obtained 3-4 cm from the macroscopic tumor) were obtained from patients (all female) with breast cancer who underwent surgical resection at Shanghai Ninth People's Hospital from March 2013 to December 2015 (Table SI). Adjacent breast tissues were confirmed as non tumoral by conventional histopathological analysis. All patients had not been diagnosed with additional co-morbidities or other types of cancer. The clinic pathological characteristics of the patients are presented in Table SI. Written informed consent was obtained from all participants. The present study was approved by the Ethics Committee of Shanghai Ninth People's Hospital (approval no. 2016-147-T96).

Cell lines. Human BCSCs were isolated and maintained as previously described (30,31). Briefly, human breast tumour cells were digested with collagenase and strained using a 40-μm filter. $CD44^+CD24^-$ cells were further sorted via fluorescence-activated cell sorting using anti-CD44 (cat. no. 75122; 1:100) and anti-CD24 (cat. no. 68390; 1:330) antibodies (each, Cell Signaling Technology, Inc.). BCSCs were maintained as spheres in ultralow attachment flasks in serum-free DMEM-F12 (Gibco; Thermo Fisher Scientific, Inc.; cat. no. 11320033) supplemented with 2% B27 (cat. no. 17504044;Gibco; Thermo Fisher Scientific, Inc.), 10 ng/ml basic fibroblast growth factor (cat. no. PHG0266; Gibco; Thermo Fisher Scientific, Inc.), 20 ng/ml epidermal growth factor (cat. no. PHG0311; Gibco; Thermo Fisher Scientific, Inc.), 5 μg/ml insulin (cat. no. I8830; Beijing Solarbio Science & Technology Co., Ltd.) and 1% penicillin-streptomycin (cat. no. 10378016; Gibco; Thermo Fisher Scientific, Inc.). The rest of the breast cancer cells (all cells other than $CD44^+CD24^-$ cells) were characterized as non-BCSCs and maintained in the same conditions as BCSCs. All cells were maintained at 37˚C with 5% CO_2.

293T cells, Lenti-X 293T cells (cat. no. 632180; Clontech Laboratories, Inc.) and MCF7 cells were maintained in DMEM (cat. no. C11995500; Gibco; Thermo Fisher Scientific, Inc.) supplemented with 10% FBS (cat. no. 30044333; Gibco; Thermo Fisher Scientific, Inc.) and 1% penicillin-streptomycin at 37˚C with 5% CO_2.

Plasmids, small interfering (si)RNAs and transfection. RAB2B expressing plasmid (pcDNA-RAB2A) was constructed by inserting the RAB2A coding sequence into vector pcDNA 3.1 (cat. no. V79020; Invitrogen; Thermo Fisher Scientific, Inc.). pcDNA 3.1 was used as the negative control for pcDNA-RAB2A. miR-376c-3p mimic (cat. no. miR10000720-1-5), negative control (NC) mimic (cat. no. miR1N0000001-1-5), si-RAB2A#1 (cat. no. siB150325183848-1-5), si-RAB2A#2 (cat. no. siB150325183922-1-5), NC siRNA (cat. no. siN0000001-1-5), miR-376c-3p inhibitor (cat. no. miR20000720-1-5) and NC inhibitor (cat. no. miR2N0000002-1-5) were purchased from Guangzhou RiboBio Co., Ltd. BCSCs in 6-well plates ($1x10^5$ cells/well) were transfected with 1 μg plasmids and 5 μl of siRNAs (20 μM) using Lipofectamine® 3000 (Invitrogen; Thermo Fisher Scientific, Inc.) according to the manufacturer's protocol. At 48 h post-transfection, cells were harvested for subsequent experimentation.

Database. miRNA profile data of breast cancer samples and healthy tissue samples were downloaded from the Gene Expression Omnibus (GEO) database (dataset no. GSE44124; www.ncbi.nlm.nih.gov/gds). The data were analyzed to identify differentially expressed miRNAs in breast cancer compared with healthy samples. Targets of miR-376c-3p were predicted using online software TargetScan (http://www.targetscan.org/vert_72/).

RNA extraction and reverse transcription-quantitative PCR (RT-qPCR). Total RNA was extracted from tissue samples and BCSCs using TRIzol® (Invitrogen; Thermo Fisher Scientific, Inc.) according to the manufacturer's protocol. To assess miR-376c-3p expression levels, the TaqMan MicroRNA Assay kit (cat. no. 4427975; Assay ID: 002122; Applied Biosystems; Thermo Fisher Scientific, Inc.) was used for reverse transcription and qPCR according to the manufacturer's protocol (primer sequences were withheld by the supplier). For RT-qPCR analysis of RAB2A mRNA, total RNA was reversed transcribed into cDNA using the GoScript Reverse Transcription system (Promega Corporation). Subsequently, qPCR was performed using FastStart Universal Master Mix (Roche) and a StepOnePlus real-time PCR system (Applied Biosystems; Thermo Fisher Scientific, Inc.). The thermocycling conditions were as follows: 40 cycles of denaturation at 94˚C for 30 sec, annealing at 58˚C for 30 sec and extension at 72˚C for 60 sec. The following primers were used for qPCR: RAB2A forward, 5'-AGTTCGGTGCTCGAATGATAAC-3' and reverse, 5'-AATACGACCTTGTGATGGAACG-3'; GAPDH forward, 5'-TGCACCACCAACTGCTTAGC-3' and reverse, 5'-GGCATGGACTGTGGTCATGAG-3'; and U6 forward, 5'-CTCGCTTCGGCAGCACA-3' and reverse, 5'-AACGCTTCACGAATTTGCGT-3'. Samples were quantified using the $2^{-\Delta\Delta Cq}$ method (32). miRNA and mRNA expression levels were normalized to the internal reference genes U6 and GAPDH, respectively.

Western blotting. Total protein was extracted using RIPA buffer (Beyotime Institute of Biotechnology), determined using BCA Protein Assay kit (Beijing Solarbio Science & Technology Co., Ltd.), and 20 μg of total protein was separated via 12% SDS-PAGE and transferred to PVDF membranes (EMD Millipore). After blocking with 5% non-fat milk for 1 h at room temperature, the membranes

were incubated with the following primary antibodies at 4˚C overnight: RAB2A (cat. no. ab154729; 1:1,000; Abcam), Ki-67 (cat. no. 9449; 1:1,000; Cell Signalling Technology, Inc.) SOX2 (cat. no. 14962; 1:1,000; Cell Signalling Technology, Inc.), OCT4 (cat. no. 2890; 1:1,200; Cell Signalling Technology, Inc.) and β-actin (cat. no. 3700; 1:1,000; Cell Signalling Technology, Inc.). Subsequently, the membranes were washed with TBST buffer (0.1% Tween-20 in TBS) and incubated with the following HRP-conjugated secondary antibodies at room temperature for 1 h: Anti-rabbit IgG (cat. no. 7074; 1:1,000; Cell Signalling Technology, Inc.) and Anti-mouse IgG (cat. no. 7076; 1:1,000; Cell Signalling Technology, Inc.). Protein bands were visualized using Pierce ECL Western Blotting substrate (Thermo Fisher Scientific, Inc.; cat. no. 32209). Bands were analysed using Image J1.50i software (National Institutes of Health).

Immunohistochemistry (IHC). Tissues were fixed in 4% paraformaldehyde for 16 h at room temperature. After fixation, tissue blocks were embedded in paraffin, sliced into 5 μM sections and affixed onto the slide. After deparaffinising and antigen retrieval, sections were blocked with blocking buffer [0.3% Triton X-100 and 5% bovine serum albumin (Beijing Solarbio Science & Technology Co., Ltd.) in PBS] for 1 h at room temperature and then incubated with the following antibodies overnight at 4˚C: RAB2A (cat. no. ab154729; 1:500; Abcam), Ki-67 (cat. no. 9449; 1:500; Cell Signalling Technology, Inc.) SOX2 (cat. no. 14962; 1:300) and OCT4 (cat. no. 2890; 1:1,200; Cell Signalling Technology, Inc.). After washing with PBST (0.1% Tween-20 in PBS), the slides were incubated with a diluted HRP-conjugated secondary antibody (Anti-rabbit IgG; cat. no. 7074; 1:1,000; Anti-mouse IgG; cat. no. 7076; 1:1,000; each, Cell Signalling Technology, Inc.) for 1 h at room temperature. After washing 5 times using PBST, DAB was added to the slide for colour developing. The slides were observed and photographed using an Olympus IX71 inverted microscope (magnification, x400; Olympus Corporation).

Luciferase reporter assay. The RAB2A 3'-untranslated region (UTR) fragment containing putative the binding site for miR-376c-3p was amplified by PCR from BCSC cDNA and inserted downstream of a luciferase gene in pmirGLO vector (Promega Corporation; cat. no. E1330). PCR primer sequences were as follows: Forward, 5'-GCCTCGAGGATTTGTTTG CCTTAATGAATAC-3' and reverse, 5'-GCTCTAGAGAGC AGTACCTGTCCTAGTTGCC-3'. The thermo cycling conditions were as follows: 30 cycles of denaturation at 94˚C for 30 sec, annealing at 56˚C for 30 sec and extension at 72˚C for 60 sec. Phusion™ High-Fidelity DNA Polymerase was utilized for PCR (Thermo Fisher Scientific, Inc.; cat. no. F530S). The seed-sequence mutation was generated by site-directed point mutagenesis. 293T cells ($5x10^4$) in a 24-well plate were co-transfected with 50 ng wild-type (WT) RAB2A-3'UTR or mutated (MUT) RAB2A-3'UTR and 20 pMol of miR-376c-3p mimic or NC-mimic. At 48 h post-transfection, luciferase activity was measured using Dual-luciferase reporter assay system (Promega Corporation; cat. no. E1910) according to the manufacturer's protocol. *Renilla* luciferase activity was used for normalization.

Mammosphere formation assay. At 48 h post-transfection, cells were harvested and adjusted to $1x10^3$ cells/ml in complete medium. Cell suspension (1 ml/well) was plated into an ultra-low-attachment 12-well plate (Corning, Inc.) and cultured for 14 days at 37˚C. Mammospheres were imaged and counted using an IX71 microscope (Olympus Corporation; magnification, x400).

Cell Counting Kit-8 (CCK-8) assay. The CCK-8 assay (Sigma-Aldrich; Merck KGaA) was performed according to the manufacturer's protocol. Briefly, at 48 h post-transfection, cells were trypsinzed and seeded into a 96-well plate ($3x10^3$ cells/well). After culture for 3 days at 37˚C, 10 μl CCK-8 reagent was added to each well and incubated at 37˚C for 2 h. The absorbance of each well was measured at a wavelength of 450 nm using Enspire Multimode Plate Reader (PerkinElmer, Inc.).

Colony formation assay. At 48 h post-transfection, cells were trypsinized and seeded into a 12-well plate ($5x10^2$ cells/well). After culture for 10-12 days at 37˚C, colonies were stained with 0.01% crystal violet for 15 min at room temperature and photographed. The colonies were defined when visible by eye and counted using ImageJ1.50i software (National Institutes of Health).

Invasion assays. Invasion assays were performed using a HTS Transwell-24 system (Corning, Inc.). The Transwell inserts were coated with Matrigel (BD Biosciences) for 20 min at room temperature. At 48 h post-transfection, cells were collected after trypsin digestion. Subsequently, cells ($1x10^5$) in 200 μl serum-free medium were plated into the upper chamber. Medium (300 μl) supplemented with 10% FBS was plated into the lower chamber. After incubation for 24 h at 37˚C, non-invading cells on the upper surface of the inserts were gently removed with a cotton swab. Invading cells were fixed with 50% methanol for 10 min at room temperature and stained with 0.01% crystal violet for 15 min at room temperature. Invasive cells were imaged using an Olympus IX71 inverted microscope (Olympus Corporation; magnification, x400) and analysed using ImageJ1. 50i software (National Institutes of Health).

Lentivirus. To construct pLVX-miR-376c-3p, the following oligonucleotides were designed: miR376c-Top, 5'-GAACAT AGAGGAAATTCCACGTTTCAAGAGAACGTGGAATTT CCTCTATGTTTTTTTT-3'; miR376c-Bottom, 5'-AAAAAA AACATAGAGGAAATTCCACGTTCTCTTGAAACG TGGAATTTCCTCTATGTTC-3'. The oligonucleotides were annealed (72˚C for 2 min, 37˚C for 2 min, 25˚C for 2 min and stored on ice) and then cloned into pLVX-shRNA1 (Clontech Laboratories, Inc.; cat. no. 632177) according to the manufacturer's protocol. To generate the lentivirus, $5x10^5$ Lenti-X 293T cells (Clontech Laboratories, Inc.; cat. no. 632180) were seeded into a 10-cm dish 20 h prior to transfection. A total of 15 μl Lenti-X HT Packaging Mix (Clontech Laboratories, Inc.; cat. no. 631247) and 3 μg pLVX-miR-376c-3p (pLVX-shRNA1 vector as control) were transfected into Lenti-X 293T cells using lipofectamine®3000 according to manufacturer's protocol. At 48 h post-transfection, the lentivirus-containing

supernatants were harvested, filtered through 0.45 μm filters, and stocked in aliquots at -80˚C.

Transduction of letivirus. BCSCs ($5x10^5$ cells) were seeded into 10-cm dishes 20 h prior to transduction. Lentivirus stock was diluted 3 folds using fresh medium for BCSC culture. BCSC culture supernatant was replaced with 5 ml of viral supernatant in the presence of 4 μg/ml polybrene (Sigma-Aldrich; Merck KGaA; cat. no. TR-1003-G). After incubating at 37˚C for 6 h, the viral supernatant was replaced with fresh medium. At 48 h after supernatant replenishment, cells were split 1:5 into BCSC culture medium containing 1 μg/ml puromycin (Gibco; Thermo Fisher Scientific, Inc.; cat. no. A1113803). After selection for 5 days, cells were harvested for inoculation.

Xenograft mouse model. A total of 12 female NOD/SCID mice (age, 4-6 weeks; weight: 18-22 g) were purchased from Shanghai Laboratory Animal Center. The mice were randomly separated into two groups: i) One group were injected with BCSCs infected with lentivirus vector; and ii) the other group were injected with cells infected with lentivirus expressing miR-376-3p. BCSCs ($5x10^5$) mixed with Matrigel (1:1) were injected into the mouse mammary fat pad. Tumour volume was measured on 18, 21, 24, 27 and 30 days post-inoculation. On day 30 post-inoculation, mice were anesthetized in a chamber containing 2.5% isoflurane in oxygen prior to sacrifice by cervical dislocation. Subsequently, the tumours were excised, weighed and subjected to IHC. The present study was approved by the Animal Care and Use Committee of Shanghai Ninth People's Hospital Affiliated to Shanghai Jiao Tong University School of Medicine (Approval no. 2016-147-T96).

Statistical analysis. All experiments were repeated at least three times. Data are presented as the mean ± standard deviation. Statistical analyses were conducted using GraphPad Prism software (version 6.0; GraphPad Software, Inc.). Comparisons between two groups were analysed using the Student's t-test. Comparisons among multiple groups were analysed using one-way ANOVA followed by Bonferroni's test. The correlation between RAB2A and miR-376c-3p was assessed by conducting Pearson's correlation analysis. $P<0.05$ was considered to indicate a statistically significant difference.

Results

Aberrant expression of miR-376c-3p and RAB2A in breast cancer. To identify miRNAs that participate in breast cancer tumorigenesis, the miRNA profile data of breast cancer tumours and adjacent non-cancerous tissues were obtained from the GEO database. Bioinformatics analysis identified 20 downregulated and 3 upregulated miRNAs in breast cancer tumours (Fig. 1A). Among the miRNAs, miR-376c-3p has been reported to participate in the development of several types of cancer (22-27), and is downregulated in breast cancer (33-36). However, how miRNAs affect breast cancer progression is not completely understood. Therefore, miR-376c-3p was selected for further investigation in the present study. A total of 60 paired breast cancer tumour samples and adjacent non-cancerous tissues were obtained from patients with breast cancer who underwent surgical resection. The RT-qPCR results indicated that the expression level of miR-376c-3p in breast cancer tumour tissues was significantly decreased compared with healthy tissues (Fig. 1B). The correlation analysis indicated that low miR-376c-3p expression was significantly correlated with lymph node metastasis (P=0.002; Table SI), which was consistent with previous studies that demonstrated that miR-376c-3 served as a cancer suppressor (22-25). Among the potential targets of miR-376c-3ppredicted using online software TargetScan (http://www.targetscan.org/vert_72/), RAB2A has been reported to be involved in breast cancer development (28,29). mRNA expression levels of RAB2A were significantly higher in breast cancer tissues compared with healthy tissues (Fig. 1B). Moreover, the expression level of miR-376c-3p was negatively correlated with the expression level of RAB2A in breast cancer tumours (Fig. 1C). The IHC results suggested that the protein level of RAB2A in breast cancer tumors was markedly higher compared with healthy tissues (Fig. 1D). Overall, the results indicated that miR-376c-3p was downregulated in breast cancer, and RAB2A may be regulated by miR-376c-3p in breast cancer.

Dysregulation of miR-376c-3p and RAB2A in BCSCs. To investigate the role of miR-376c-3p in the tumorigenesis of breast cancer, $CD44^+CD24^-$ cells were isolated from breast cancer tumours (Fig. 2A), which were characterized as BSCSs. Stem cell-associated proteins OCT4 and SOX2 were expressed at significantly higher levels in BCSCs compared with MCF7 breast cancer cells (Fig. 2B). Breast cancer cells (MCF7, non-BCSCs and BCSCs) expressed significantly lower levels of miR-376c-3p and significantly higher levels of RAB2A compared with MCF-10A normal breast epithelial cells (Fig. 2C). The western blotting results indicated that the protein expression level of RAB2A in BCSCs was significantly higher compared with normal cells, MCF7 cells and non-BCSCs (Fig. 2D). The dysregulation of miR-376c-3p and RAB2A in breast cancer tumours suggested they may serve a role in BCSCs.

miR-376c-3p targets RAB2A mRNA for degradation. The predicted targeted sequence of RAB2A by miR-376c-3p is presented in Fig. 3A. To verify the interaction between RAB2A and miR-376c-3p, luciferase reporter constructs were constructed by inserting the 3'UTR sequences of RAB2A downstream of a luciferase gene. 293T cells were co-transfected with the reporter plasmid and miR-376c-3p mimic or NC-mimic. The results indicated that miR-376c-3p mimic significantly reduced the luciferase activity of WT RAB2A-3'UTR compared with NC-mimic (Fig. 3B). By contrast, miR-376c-3p mimic did not significantly alter the luciferase activity of MUT RAB2A-3'UTR compared with NC-mimic (Fig. 3B), indicating the specificity of the target sequence. The effect of miR-376c-3p on endogenous RAB2A expression in BCSCs was also examined. RAB2A was expressed at lower levels in miR-376c-3p mimic-transfected cells compared with the NC-mimic group, but expressed at higher levels in miR-376c-3p inhibitor-transfected cells compared with the NC inhibitor (Fig. 3C). The western blotting results indicated that RAB2A protein expression was decreased in miR-376c-3p mimic-transfected BCSCs compared with the NC-mimic group, and increased in miR-376c-3p inhibitor-transfected cells compared with the NC

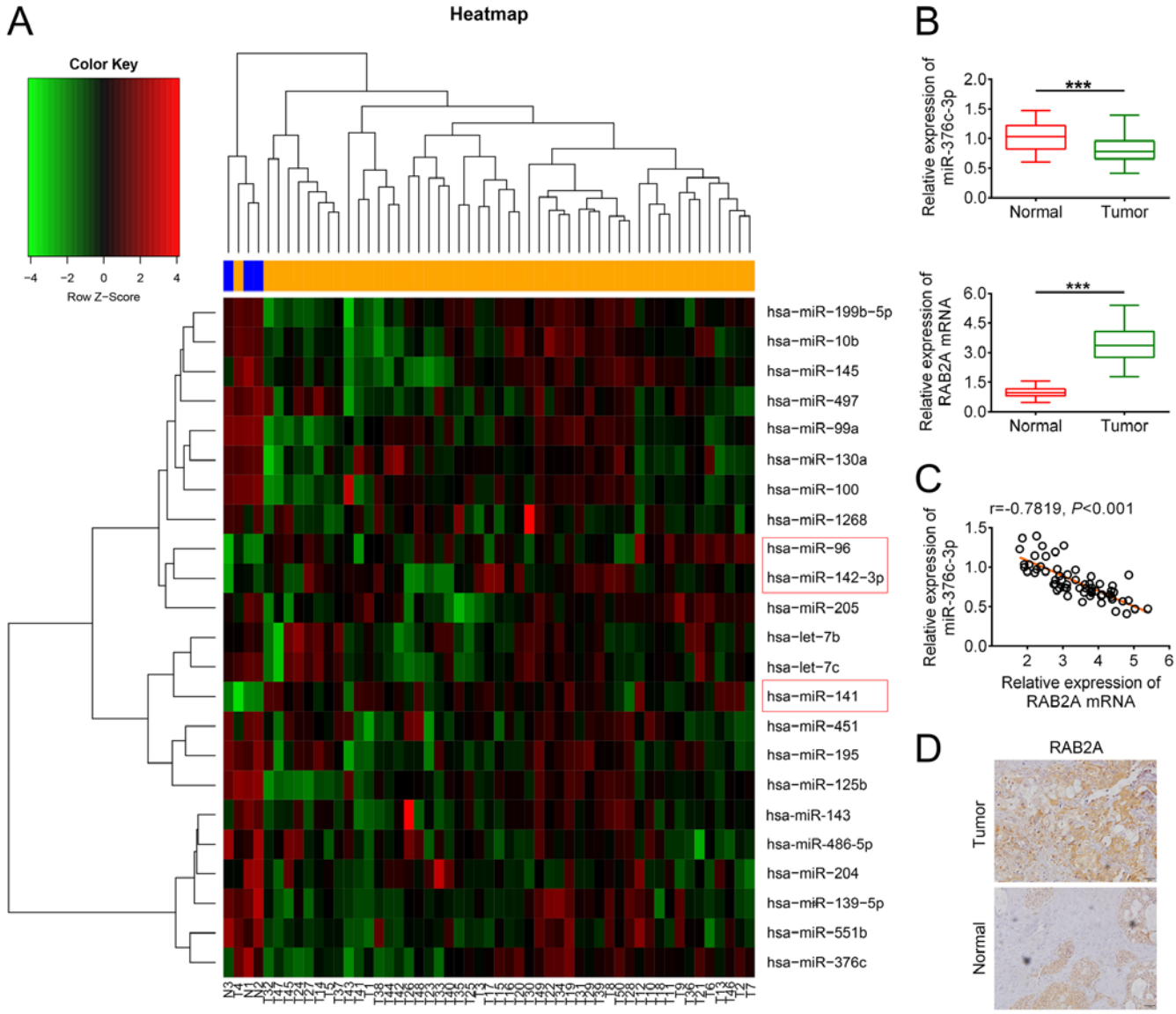

Figure 1. Expression levels of miR-376c-3p and RAB2A in breast cancer tumors. (A) Hierarchical cluster of the miRNA profile data. The heat map presents the 3 most upregulated miRNAs and the 20 most downregulated miRNAs in breast cancer tissues. Red, green and black represents upregulated, downregulated and no change, respectively. Blue indicates healthy samples and orange indicates tumor samples. (B) Reverse transcription-quantitative PCR analysis of miR-376c-3p and RAB2A expression levels in 60 paired breast cancer tumor and adjacent non-cancerous tissues. (C) Pearson's correlation analysis of miR-376c-3p and RAB2A expression levels in 60 breast cancer tumors. (D) Immunohistochemical analysis of RAB2A expression in breast cancer and healthy tissues. ***P<0.001. miR/miRNA, microRNA; RAB2A, Ras-related protein Rab-2A.

inhibitor group (Fig. 3D). Collectively, the results demonstrated that miR-376c-3p targeted RAB2A and regulated RAB2A expression.

miR-376c-3p reduces stem cell population and downregulates stem cell regulatory proteins by targeting RAB2A. The observation that miR-376c-3p was downregulated in BCSCs implied that miR-376-3p may regulate BCSC fate. To determine the effect of miR-376c-3p on BCSCs, BCSCs were transfected with miR-376-3p mimic and the expression of the BCSC surface markers CD44 and CD24 was examined via flow cytometry. Compared with NC-mimic, miR-376c-3p mimic reduced the proportion of $CD44^+CD24^-$ cells from 95.6 to 38.2% (Fig. 4A), indicating a decrease in BCSCs. To prove functional relevance of RAB2A regulation by miR-376c-3p, cells were co-transfected with RAB2A-expressing plasmid pcDNA-RAB2A and miR-376c-3p mimic. Expression of RAB2A in pcDNA-RAB2A-transfected BCSCs is presented in Fig. S2. RAB2A overexpression reversed miR-376c-3p-mediated loss of BCSCs. Furthermore, the expression of stem cell regulatory genes OCT4 and SOX2 in miR-376c-3p-transfected BCSCs was assessed by western blotting. Compared with NC-mimic, OCT4 and SOX2 expression levels were significantly decreased by miR-376c-3p mimic, which was reversed by RAB2A overexpression (Fig. 4B). In addition, compared with NC inhibitor, miR-376c-3p inhibitor significantly increased the expression of OCT4 and SOX2, which was reversed by RAB2A siRNA (Figs. 4C and S1). si-RAB2A#1 was used in Figs. 4 and 5, as it demonstrated a more prominent silencing effect. Collectively, the results demonstrated that miR-376c-3p reduced the stem cell population and downregulated stem cell regulatory proteins by targeting RAB2A.

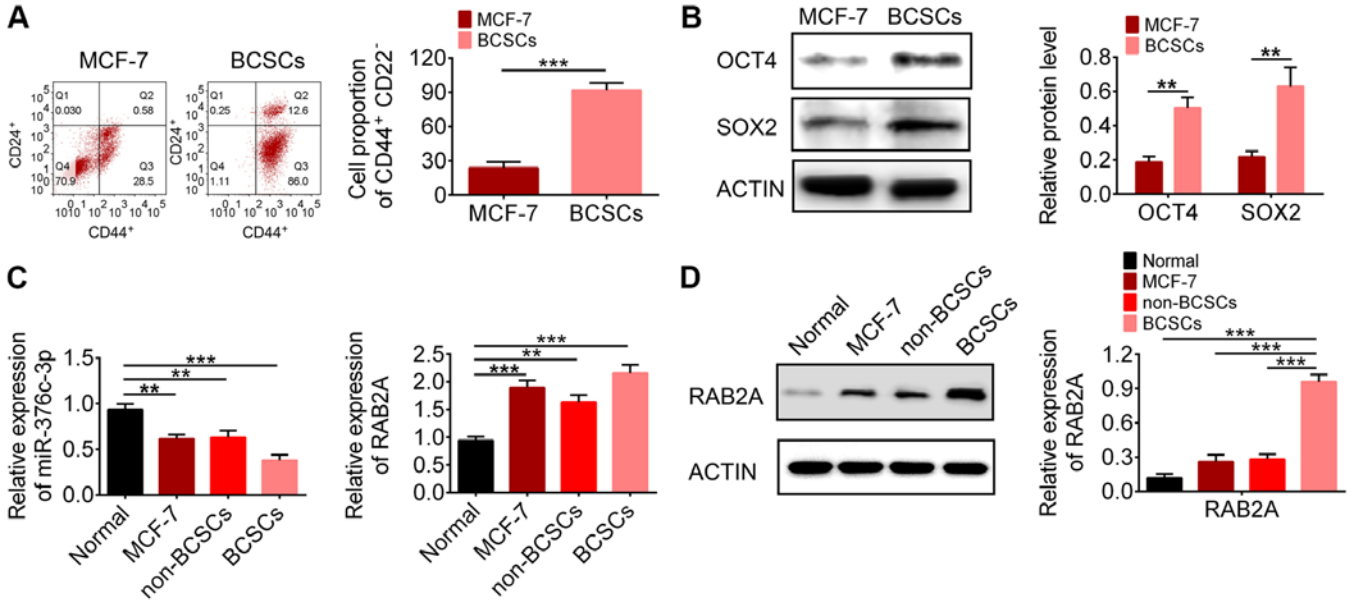

Figure 2. Expression levels of miR-376c-3p and RAB2A in BCSCs. (A) Flow cytometry analysis of the proportion of CD44+CD24- cells. (B) Protein expression levels of stem cell markers OCT4 and SOX2 in MCF-7 cells and BCSCs. (C) Reverse transcription-quantitative PCR analysis of miR-376c-3p and RAB2A expression levels in MCF-10A cells, MCF-7 cells, non-BCSCs and BCSCs. (D) Protein expression levels of RAB2A in MCF-10A cells, MCF-7 cells, non-BCSCs and BCSCs. **P<0.01 and ***P<0.001. miR, microRNA; RAB2A, Ras-related protein Rab-2A; BCSC, breast cancer stem cell; CD, cluster of differentiation; OCT4, octamer-binding transcription factor 4; SOX2, SRY-box transcription factor 2.

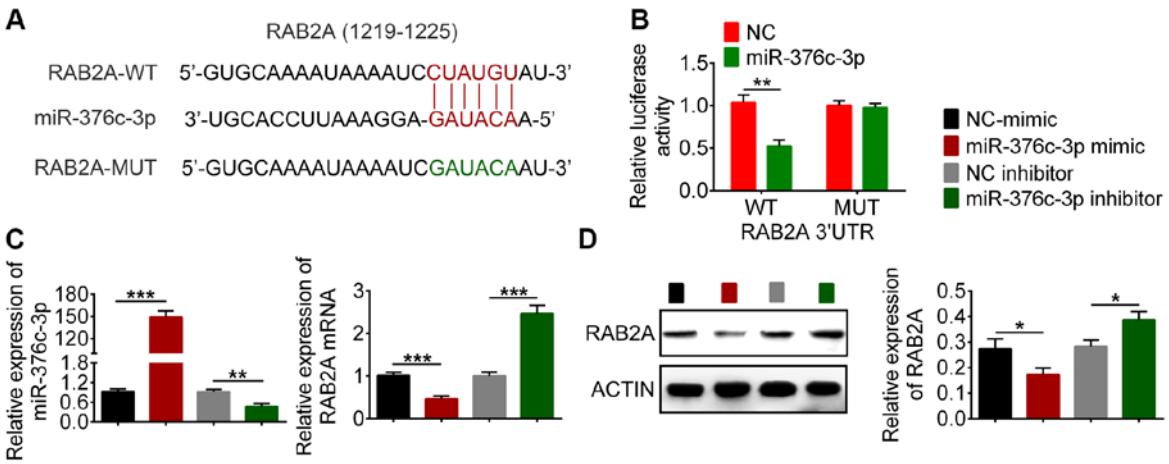

Figure 3. miR-376-3p targets RAB2A in BCSCs. (A) The predicted target sequence of RAB2A mRNA by miR-376-3p. (B) Luciferase activity of 293T cells co-transfected with WT RAB2A-3'UTR or MUT RAB2A-3'UTR and NC-mimic or miR-376c-3p mimic. (C) Effect of miR-376c-3p overexpression and knockdown on RAB2A mRNA expression levels. (D) Effect of miR-376c-3p overexpression and knockdown on RAB2A protein expression levels. *P<0.05, **P<0.01 and ***P<0.001. miR, microRNA; RAB2A, Ras-related protein Rab-2A; BCSC, breast cancer stem cell; WT, wild-type; MUT, mutated; UTR, untranslated region; NC, negative control.

miR-376c-3p regulates BCSC tumorigenic properties via RAB2A. To further explore the role of miR-376c-3p in tumorigenesis, gain- and loss-of-function experiments were conducted by transfecting BCSCs with miR-376c-3p mimic or miR-376c-3p inhibitor. A mammosphere assay was performed to assess the effect of miR-376c-3p on BCSC self-renewal. miR-376c-3p mimic significantly reduced the sphere number compared with NC-mimic, whereas miR-376c-3p inhibitor significantly increased the sphere number compared with NC inhibitor, which suggested that miR-376c-3p had an inhibitory effect on BCSC self-renewal (Fig. 5A). Subsequently, CCK-8 and colony formation assays were conducted to examine the effect of miR-376c-3p on cell proliferation. The results indicated that miR-376c-3p mimic significantly inhibited BCSC proliferation compared with NC-mimic, whereasmiR-376c-3p inhibitor significantly enhanced BCSC proliferation compared with NC inhibitor (Fig. 5B and C). Moreover, BCSC invasion was examined using a cell invasion assay. miR-376c-3p overexpression significantly inhibited BCSC invasion compared with NC-mimic, whereas miR-376c-3p knockdown significantly enhanced BCSC invasion compared with NC inhibitor (Fig. 5D). RAB2A overexpression reversed miR-376c-3p mimic-induced effects and RAB2A knockdown reversed miR-376c-3p inhibitor-induced effects (Fig. 5A-D), indicating

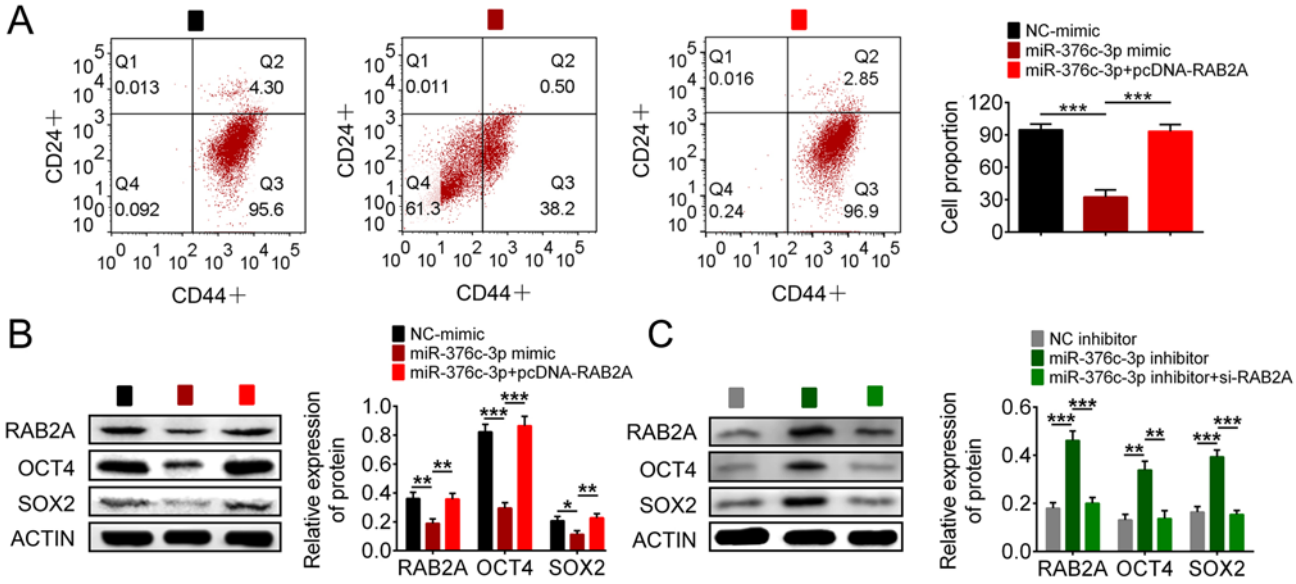

Figure 4. miR-376-3p reduces the stem cell population and downregulates stem cell regulatory proteins by targeting RAB2A. (A) Flow cytometry analysis of the proportion of CD44+CD24- cells. The effect of (B) miR-376c-3p mimic, pcDNA-RAB2A, (C) miR-376c-3p inhibitor and si-RAB2A on RAB2A, OCT4 and SOX2 expression levels. *P<0.05, **P<0.01 and ***P<0.001. miR, microRNA; RAB2A, Ras-related protein Rab-2A; CD, cluster of differentiation; si, small interfering RNA; OCT4, octamer-binding transcription factor 4; SOX2, SRY-box transcription factor 2; NC, negative control.

that miR-376c-3p targeted RAB2A to inhibit the tumorigenic properties of BCSCs.

miR-376c-3p overexpression inhibits breast cancer growth in a mouse xenograft model. The effect of miR-376c-3p overexpression on tumour formation in a mouse model was assessed. The expression levels of miR-376c-3p and RAB2A were measured in lentivirus-infected BCSCs (Fig. 6A and B). RAB2A expression was significantly downregulated in PLVX-miR-376c-3p-infected BCSCs compared with PLVX-vector-infected BCSCs (Fig. 6B). Subsequently, the infected cells were inoculated into the mammary fat pad of 4-6 week old female NOD/SCID mice and tumour growth was monitored for 30 days. On day 30 post-inoculation, the mice were sacrificed and the tumours were excised. The tumour volume and weight in the miR-376c-3p group was significantly reduced compared with the vector group (Fig. 6C). The expression levels of Ki-67, SOX2 and OCT4 in the tumours of the miR-376c-3p group were markedly lower compared with the vector group (Fig. 6D). The results demonstrated that miR-376c-3p overexpression inhibited breast cancer growth in a mouse xenograft model.

Discussion

miRNAs are common gene regulators in cellular signalling pathways that are implicated in cancer progression (7,8). A number of miRNAs have been reported to regulate BCSC stemness (6,37). let-7 regulates BCSC self-renewal and differentiation by targeting ras homolog family member Hand high mobility group AT-hook 2 (11). miR-200c serves a role in regulating BCSC stemness by targeting BMI1 proto-oncogene, polycomb ring finger and programmed cell death 10 (12,13). miR-93 expression depletes the BCSC population and inhibits tumor development (14). miR-600 targets SCD1 and inhibits WNT signalling, leading to a reduction in BCSC self-renewal (16).

The present study identified 23 differentially expressed miRNAs in breast cancer tissues compared with healthy tissues by conducting miRNA microarray analysis. miR-376c-3p, which was downregulated in breast cancer tissues and BCSCs, was selected for further study. By conducting bioinformatics analysis and validation assays, RAB2A was identified as a target of miR-376c-3p. The results also indicated that miR-376c-3p and RAB2A were dysregulated in BCSCs, suggesting they may serve roles in regulating BCSC stemness. By analysing CD44 and CD24 surface marker expression levels, the results indicated that miR-376c-3p overexpression depleted the BCSC population. miR-376c-3p mimic also downregulated the expression of stem cell regulatory genes OCT4 and SOX2 compared with NC-mimic. miR-376c-3p-mediated effects were reversed by RAB2A overexpression, indicating the functional interaction between RAB2A and miR-376c-3p in BCSCs. Furthermore, functional assays indicated that, compared with NC-mimic, miR-376c-3p mimic inhibited BCSC self-renewal, proliferation and invasion, which was reversed by RAB2A overexpression. *In vivo* experiments were conducted in a mouse xenograft model that suggested miR-376c-3p overexpression inhibited breast cancer growth compared with the vector group. Collectively, the results indicated that miR-376c-3p served a role in regulating BCSC stemness by targeting RAB2A.

RAB2A is a small GTPase that serves an essential role in the membrane transport between ER and Golgi (28). Luo *et al* (28) reported that RAB2A also functions as an oncogene in breast cancer viagenomic profiling analysis. Bioinformatics analysis indicated that RAB2A is aberrantly activated in human cancer and associated with poor prognosis (28). Mechanistically, RAB2A interacts with and

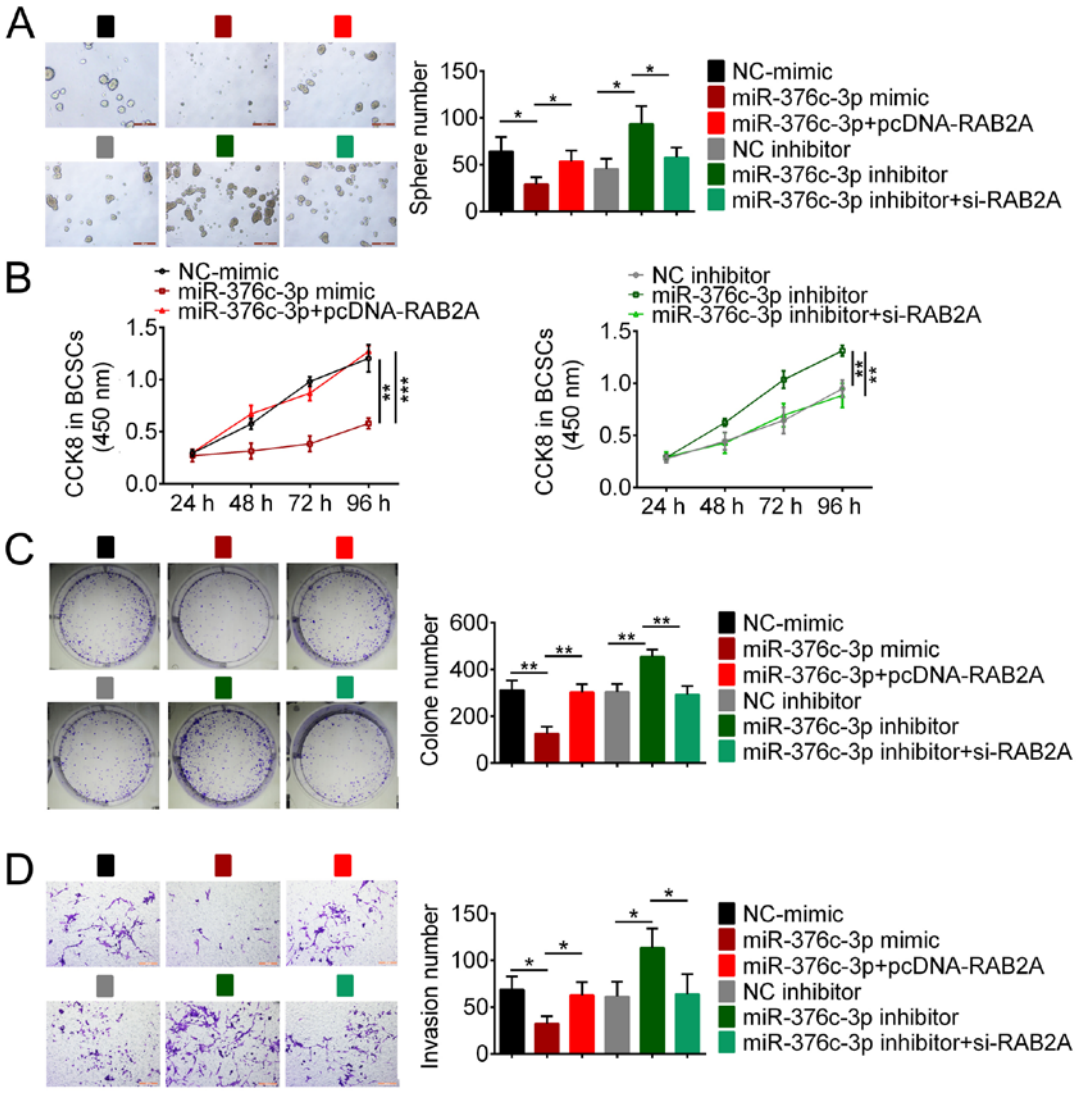

Figure 5. miR-376-3p inhibits BCSC self-renewal, proliferation and invasion by targeting RAB2A. (A) Mammosphere assay. Cell proliferation was assessed by conducting (B) CCK-8 and (C) colony formation assays. (D) Cell invasion was assessed by performing a Transwell invasion assay. *P<0.05, **P<0.01 and ***P<0.001. miR, microRNA; BCSC, breast cancer stem cell; RAB2A, Ras-related protein Rab-2A; CCK-8, Cell Counting Kit-8; NC, negative control; si, small interfering RNA.

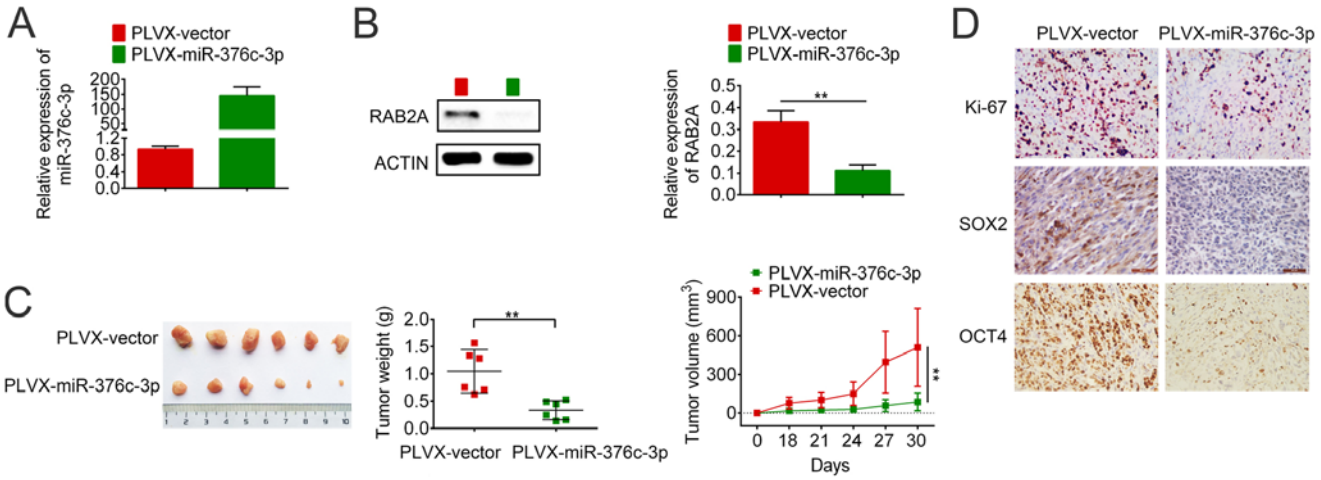

Figure 6. miR-376-3p inhibits breast cancer growth in mice. (A) miR-376c-3p and (B) RAB2A expression in BCSCs infected with PLVX-vector (PLVX-shRNA1 vector) virus or PLVX-miR-376c-3p virus. (C) PLVX-vector- or PLVX-miR-376c-3p-infected BCSCs were inoculated into the mammary fat pad of 4-6 weeks old female NOD/SCID mice. Tumour volume and weight were measured. (D) The expression of Ki-67, SOX2 and OCT4 in mouse xenograft breast tumour tissues were detected via immunohistochemistry (magnification, x400). **P<0.01. miR, microRNA; RAB2A, Ras-related protein Rab-2A; BCSC, breast cancer stem cell; SOX2, SRY-box transcription factor 2; OCT4, octamer-binding transcription factor 4.

prevents the inactivation of ERK1/2, leading to upregulation of zinc finger E-box binding homeobox 1 and nuclear translocation of β-catenin (28). Abnormal activation of RAB2A ultimately promotes BCSC expansion and tumorigenicity (28). In another study, Kajiho *et al* (29) demonstrated that RAB2A regulates the trafficking of matrix metallopeptidase 14 and E-cadherin, thereby enhancing breast cancer invasion. The study also indicated that elevated expression of RAB2A is strongly linked to metastatic recurrence of breast cancer in patients, which suggests that RAB2A may serve as a useful prognosis biomarker in breast cancer. RAB2A was also reported to be required for autophagosome clearance in breast cancer cells (38). In the present study, the results indicated that RAB2A expression was regulated by miR-376c-3p, and the miRNA/target axis modulated BCSC fate and properties. miR-376c-3p also targets other genes, such as RUNX2 (22), BAD and Smad4 (23); therefore, whether these genes affect BCSC stemness requires further investigation.

In summary, the present study indicated that miR-376c-3p was associated with regulating BCSC stemness. Compared with NC-mimic, miR-376c-3p overexpression reduced the $CD44^+CD24^-$ population and downregulated stem cell regulatory genes. Additionally, miR-376c-3p overexpression inhibited BCSC self-renewal, proliferation and invasion, and suppressed tumour growth in a mouse xenograft model. miR-376c-3p performed the aforementioned biological functions by targeting RAB2A. The present study identified a potential mechanism underlying BCSC stemness regulation and suggested that miR-376c-3p may serve as a therapeutic target for breast cancer.

Acknowledgements

Not applicable.

Funding

Not applicable.

Availability of data and materials

The datasets used and/or analyzed during the present study are available from the corresponding author on reasonable request.

Authors' contributions

FZ and YC conceived and designed the study. MZ analyzed and interpreted the data. WP and BT performed the experiments. All authors read and approved the final manuscript.

Ethics approval and consent to participate

The present study was approved by the Ethics Committee of Shanghai Ninth People's Hospital (approval no. 2016-147-T96). Written informed consent was obtained from all participants.

Patient consent for publication

Not applicable.

Competing interests

The authors declare that they have no competing interests.

References

1. Kreso A and Dick JE: Evolution of the cancer stem cell model. Cell Stem Cell 14: 275-291, 2014.
2. Visvader JE and Lindeman GJ: Cancer stem cells: Current status and evolving complexities. Cell Stem Cell 10: 717-728, 2012.
3. Richie RC and Swanson JO: Breast cancer: A review of the literature. J Insurance Med 35: 85-101, 2003.
4. Siegel RL, Miller KD and Jemal A: Cancer statistics, 2018. CA Cancer J Clin 68: 7-30, 2018.
5. Bray F, Ferlay J, Soerjomataram I, Siegel RL, Torre LA and Jemal A: Global cancer statistics 2018: GLOBOCAN estimates of incidence and mortality worldwide for 36 cancers in 185 countries. CA Cancer J Clin 68: 394-424, 2018.
6. Shimono Y, Mukohyama J, Nakamura S and Minami H: MicroRNA regulation of human breast cancer stem cells. J Clin Med 5: 2, 2016.
7. Hayes J, Peruzzi PP and Lawler S: MicroRNAs in cancer: Biomarkers, functions and therapy. Trends Mol Med 20: 460-469, 2014.
8. Peng Y and Croce CM: The role of MicroRNAs in human cancer. Signal Transduct Target Ther 1: 15004, 2016.
9. Takahashi RU, Miyazaki H and Ochiya T: The role of microRNAs in the regulation of cancer stem cells. Front Genet 4: 295, 2014.
10. Garg M: Emerging role of microRNAs in cancer stem cells: Implications in cancer therapy. World J Stem Cells 7: 1078-1089, 2015.
11. Yu F, Yao H, Zhu P, Zhang X, Pan Q, Gong C, Huang Y, Hu X, Su F, Lieberman J and Song E: Let-7 regulates self renewal and tumorigenicity of breast cancer cells. Cell 131: 1109-1123, 2007.
12. Shimono Y, Zabala M, Cho RW, Lobo N, Dalerba P, Qian D, Diehn M, Liu H, Panula SP, Chiao E, *et al*: Downregulation of miRNA-200c links breast cancer stem cells with normal stem cells. Cell 138: 592-603, 2009.
13. Feng ZM, Qiu J, Chen XW, Liao RX, Liao XY, Zhang LP, Chen X, Li Y, Chen ZT and Sun JG: Essential role of miR-200c in regulating self-renewal of breast cancer stem cells and their counterparts of mammary epithelium. BMC Cancer 15: 645, 2015.
14. Liu S, Patel SH, Ginestier C, Ibarra I, Martin-Trevino R, Bai S, McDermott SP, Shang L, Ke J, Ou SJ, *et al*: MicroRNA93 regulates proliferation and differentiation of normal and malignant breast stem cells. PLoS Genet 8: e1002751, 2012.
15. Taube JH, Malouf GG, Lu E, Sphyris N, Vijay V, Ramachandran PP, Ueno KR, Gaur S, Nicoloso MS, Rossi S, *et al*: Epigenetic silencing of microRNA-203 is required for EMT and cancer stem cell properties. Sci Rep 3: 2687, 2013.
16. El Helou R, Pinna G, Cabaud O, Wicinski J, Bhajun R, Guyon L, Rioualen C, Finetti P, Gros A, Mari B, *et al*: miR-600 Acts as a Bimodal switch that regulates breast cancer stem cell fate through WNT signaling. Cell Rep 18: 2256-2268, 2017.
17. Ma S, Tang KH, Chan YP, Lee TK, Kwan PS, Castilho A, Ng I, Man K, Wong N, To KF, *et al*: miR-130b promotes CD133(+) liver tumor-initiating cell growth and self-renewal via tumor protein 53-induced nuclear protein 1. Cell Stem Cell 7: 694-707, 2010.
18. Liu C, Kelnar K, Liu B, Chen X, Calhoun-Davis T, Li H, Patrawala L, Yan H, Jeter C, Honorio S, *et al*: The microRNA miR-34a inhibits prostate cancer stem cells and metastasis by directly repressing CD44. Natu Med 17: 211-215, 2011.
19. Bu P, Chen KY, Chen JH, Wang L, Walters J, Shin YJ, Goerger JP, Sun J, Witherspoon M, Rakhilin N, *et al*: A microRNA miR-34a-regulated bimodal switch targets Notch in colon cancer stem cells. Cell Stem Cell 12: 602-615, 2013.
20. Hwang WL, Jiang JK, Yang SH, Huang TS, Lan HY, Teng HW, Yang CY, Tsai YP, Lin CH, Wang HW and Yang MH: MicroRNA-146a directs the symmetric division of Snail-dominant colorectal cancer stem cells. Nat Cell Biol 16: 268-280, 2014.
21. Wang H, Sun T, Hu J, Zhang R, Rao Y, Wang S, Chen R, McLendon RE, Friedman AH, Keir ST, *et al*: miR-33a promotes glioma-initiating cell self-renewal via PKA and NOTCH pathways. J Clin Invest 124: 4489-4502, 2014.

22. Chang WM, Lin YF, Su CY, Peng HY, Chang YC, Lai TC, Wu GH, Hsu YM, Chi LH, Hsiao JR, *et al*: Dysregulation of RUNX2/Activin-A Axis upon miR-376c downregulation promotes lymph node metastasis in head and neck squamous cell carcinoma. Cancer Res 76: 7140-7150, 2016.
23. Tu L, Zhao E, Zhao W, Zhang Z, Tang D, Zhang Y, Wang C, Zhuang C and Cao H: Hsa-miR-376c-3p regulates gastric tumor growth both in vitro and in vivo. Biomed Res Int 2016: 9604257, 2016.
24. Wang K, Jin J, Ma T and Zhai H: MiR-376c-3p regulates the proliferation, invasion, migration, cell cycle and apoptosis of human oral squamous cancer cells by suppressing HOXB7. Biomed Pharmacother 91: 517-525, 2017.
25. Bhavsar SP, Lokke C, Flaegstad T and Einvik C: Hsa-miR-376c-3p targets Cyclin D1 and induces G1-cell cycle arrest in neuroblastoma cells. Oncol Lett 16: 6786-6794, 2018.
26. Wang Y, Chang W, Chang W, Chang X, Zhai S, Pan G and Dang S: MicroRNA-376c-3p Facilitates human hepatocellular carcinoma progression via repressing at-rich interaction domain 2. J Cancer 9: 4187-4196, 2018.
27. Zhang YH, Fu J, Zhang ZJ, Ge CC and Yi Y: LncRNA-LINC00152 down-regulated by miR-376c-3p restricts viability and promotes apoptosis of colorectal cancer cells. Am J Transl Res 8: 5286-5297, 2016.
28. Luo ML, Gong C, Chen CH, Hu H, Huang P, Zheng M, Yao Y, Wei S, Wulf G, Lieberman J, *et al*: The Rab2A GTPase promotes breast cancer stem cells and tumorigenesis via Erk signaling activation. Cell Rep 11: 111-124, 2015.
29. Kajiho H, Kajiho Y, Frittoli E, Confalonieri S, Bertalot G, Viale G, Di Fiore PP, Oldani A, Garre M, Beznoussenko GV, *et al*: RAB2A controls MT1-MMP endocytic and E-cadherin polarized Golgi trafficking to promote invasive breast cancer programs. EMBO Reps 17: 1061-1080, 2016.
30. Lin X, Chen W, Wei F, Zhou BP, Hung MC and Xie X: POMC maintains tumor-initiating properties of tumor tissue-derived long-term-cultured breast cancer stem cells. Int J Cancer 140: 2517-2525, 2017.
31. Lin X, Chen W, Wei F, Zhou BP, Hung MC and Xie X: Nanoparticle delivery of miR-34a Eradicates Long-term-cultured breast cancer stem cells via targeting C22ORF28 directly. Theranostics 7: 4805-4824, 2017.
32. Livak KJ and Schmittgen TD: Analysis of relative gene expression data using real-time quantitative PCR and the 2(-Delta Delta C(T)) method. Methods 25: 402-408, 2001.
33. Huo D, Clayton WM, Yoshimatsu TF, Chen J and Olopade OI: Identification of a circulating microRNA signature to distinguish recurrence in breast cancer patients. Oncotarget 7: 55231-55248, 2016.
34. Zhang L, Chen Y, Wang H, Zheng X, Li C and Han Z: miR-376a inhibits breast cancer cell progression by targeting neuropilin-1 NR. OncoTargets Ther 11:5293-5302, 2018.
35. van Schooneveld E, Wildiers H, Vergote I, Vermeulen PB, Dirix LY and Van Laere SJ: Dysregulation of microRNAs in breast cancer and their potential role as prognostic and predictive biomarkers in patient management. Breast Cancer Res 17: 21, 2015.
36. Cuk K, Zucknick M, Heil J, Madhavan D, Schott S, Turchinovich A, Arlt D, Rath M, Sohn C, Benner A, *et al*: Circulating microRNAs in plasma as early detection markers for breast cancer. Int J Cancer 132: 1602-1612, 2013.
37. Fan X, Chen W, Fu Z, Zeng L, Yin Y and Yuan H: MicroRNAs, a subpopulation of regulators, are involved in breast cancer progression through regulating breast cancer stem cells. Oncol Lett 14: 5069-5076, 2017.
38. Lőrincz P, Tóth S, Benkő P, Lakatos Z, Boda A, Glatz G, Zobel M, Bisi S, Hegedűs K, Takáts S, *et al*: Rab2 promotes autophagic and endocytic lysosomal degradation. J Cell Biol 216: 1937-1947, 2017.